

Article

A Deep Learning Integrated Lee–Carter Model

Andrea Nigri ^{1,*}, Susanna Levantesi ¹, Mario Marino ¹, Salvatore Scognamiglio ² and Francesca Perla ³

¹ Department of Statistics, Sapienza University of Rome, Viale Regina Elena, 295/G, 00161 Rome, Italy; susanna.levantesi@uniroma1.it (S.L.); m.marino@uniroma1.it (M.M.)

² Department of Economic and Legal Studies, University of Naples “Parthenope”, 13, Generale Parisi Street, 80132 Naples, Italy; salvatore.scognamiglio@uniparthenope.it

³ Department of Business and Quantitative Studies, University of Naples “Parthenope”, 13, Generale Parisi Street, 80132 Naples, Italy; francesca.perla@uniparthenope.it

* Correspondence: andrea.nigri@uniroma1.it

Received: 31 December 2018; Accepted: 13 March 2019; Published: 16 March 2019

Abstract: In the field of mortality, the Lee–Carter based approach can be considered the milestone to forecast mortality rates among stochastic models. We could define a “Lee–Carter model family” that embraces all developments of this model, including its first formulation (1992) that remains the benchmark for comparing the performance of future models. In the Lee–Carter model, the κ_t parameter, describing the mortality trend over time, plays an important role about the future mortality behavior. The traditional ARIMA process usually used to model κ_t shows evident limitations to describe the future mortality shape. Concerning forecasting phase, academics should approach a more plausible way in order to think a nonlinear shape of the projected mortality rates. Therefore, we propose an alternative approach the ARIMA processes based on a deep learning technique. More precisely, in order to catch the pattern of κ_t series over time more accurately, we apply a Recurrent Neural Network with a Long Short-Term Memory architecture and integrate the Lee–Carter model to improve its predictive capacity. The proposed approach provides significant performance in terms of predictive accuracy and also allow for avoiding the time-chunks’ a priori selection. Indeed, it is a common practice among academics to delete the time in which the noise is overflowing or the data quality is insufficient. The strength of the Long Short-Term Memory network lies in its ability to treat this noise and adequately reproduce it into the forecasted trend, due to its own architecture enabling to take into account significant long-term patterns.

Keywords: mortality; deep learning; long short-term memory; Lee–Carter model; forecasting

1. Introduction

Mortality contributes significantly to population dynamics and is crucial in many fields such as economy, demography and social sciences. Since the beginning of the nineteenth century, life expectancy has shown a continuous growth in developed countries (at a steady pace since the end of the Second World War), often at a more rapid rate than expected according to forecasts (Oeppen and Vaupel (2002)). This has created financial challenges for life insurers, pension plans and social security schemes involving benefits related to illness, death or survival of people. Mortality forecasting is then considered a key challenge for these entities.

Presently, refined techniques to forecast future mortality are becoming common among actuaries to treat longevity risk as well as to obtain more accurate prediction of life expectancy. In the context of extrapolative stochastic mortality models, the Lee and Carter (1992) model is the most frequently used, due

to some advantages like the small number of parameters compared to other models and the robustness. The model's parsimony results in a model in which mortality is stable with age, preventing the crossing of the age profile lines in the forecasting phase (see [Li et al. \(2009\)](#) for further details).

In recent years, thanks to the computational ability improvement, machine learning techniques are back on stage. Machine learning encloses many algorithms that learn from large datasets with many features and it is very useful in detecting unknown and unidentifiable patterns. Despite the increasing usage in different fields of research, machine learning applications are not so popular in demography, mainly due to the findings often considered as "black boxes" and then difficult to interpret. Moreover, machine learning algorithms are driven by data and not supported by specific hypotheses, to which demographers are more interested.

In spite of the reserve of demographers, research contributions in this field are increasing. We provide a reminder of [Hainaut \(2018\)](#), who proposes a neural network to predict and simulate mortality rates. The author uses a neural analyzer for identifying latent time processes and directly predicting mortality. This approach allows for detecting and duplicating nonlinearities observed in the evolution of log-forces of mortality. [Deprez et al. \(2017\)](#) use some machine learning techniques to improve the estimation of the log mortality rates, extended by [Levantesi and Pizzorusso \(2018\)](#) to the mortality forecasting in the Lee–Carter framework. Moreover, the recent paper of [Richman and Wüthrich \(2018\)](#) proposes a multiple-populations Lee–Carter model where parameters are estimated using neural networks. Other relevant applications of machine learning in an actuarial field can be found e.g., in [Castellani et al. \(2018\)](#) and [Gabrielli and Wüthrich \(2018\)](#).

In this paper, we use deep learning techniques in order to improve the predictive ability of the Lee–Carter model. Specifically, our approach aims to integrate the original Lee–Carter formulation introducing a Recurrent Neural Network with Long Short-Term Memory (LSTM) architecture to forecast future evolution of κ_t parameter, overcoming the limitation showed by the ARIMA processes. We think that the use of LSTM allows for obtaining mortality forecasts more coherent with the observed mortality dynamics, also in cases of nonlinear mortality trends. More precisely, the LSTM network is structured in order to elaborate long sequences of data, forming a memory able to preserve the significant relationships between data, also very distant in the sequence. In this sense, inside the time series context, LSTM allows for predicting future mortality over time considering the significant influence of the past mortality trend and adequately reproduces it into the forecasted trend. Then, strength of LSTM is then to preserve the information over time, thus preventing older signals from gradually vanishing during processing.

Therefore, the paper is focused on the forecasting of mortality trend, while the parameter estimation remains the same from [Lee and Carter \(1992\)](#). Specifically, we do not propose a new methodology for fitting the mortality surface (already introduced by [Hainaut \(2018\)](#) that uses neural networks for fitting mortality rates alternatively to the traditional singular value decomposition); instead, we introduce an innovative structure based on an LSTM network for modeling future mortality trends.

This paper is organized as follows. Section 2 describes the traditional scheme of the Lee–Carter model, Section 3 describes neural networks with particular attention to the LSTM networks. Section 4 is dedicated to the numerical application carried out on a set of six countries throughout the world and Section 5 provides conclusions.

2. Lee–Carter Model

The first version of the Lee–Carter (LC) model has been developed by the authors in 1992 using U.S. mortality data over the period 1933–1987. Several improvements of this model have been proposed over time, but the original version, together with extension provided by [Brouhns et al. \(2002\)](#), are still the benchmark for comparison with future developments.

In this paper, we refer to the first version of the model, then applying the singular value decomposition (SVD) to the logarithm of central death rates to obtain the parameters. The model has the following expression:

$$\log(m_{x,t}) = a_x + b_x \kappa_t + \epsilon_{x,t}, \quad (1)$$

where $m_{x,t}$ are the observed central death rate at age x in year t , a_x is the average age-specific pattern of mortality, b_x is the pattern of deviations from the age of profile as κ_t varies, κ_t is the time index describing mortality trend, and $\epsilon_{x,t}$ is the residual term at age x and time t . To avoid identifiability problems with the parameters, the model requires the following constraints:

$$\sum_x b_x^2 = 1; \sum_t \kappa_t = 0. \quad (2)$$

In the original LC model, the parameters are estimated by singular value decomposition (SVD) according to a two-stage procedure. Firstly, SVD is applied to the matrix of $\log(m_{x,t}) - a_x$ to find b_x and κ_t . Secondly, κ_t is refitted so that the observed number of deaths coincide with those estimated.

In the traditional LC formulation, κ_t is usually modeled by an ARIMA(0,1,0):

$$\kappa_t = \kappa_{t-1} + \delta + \epsilon_t, \quad \epsilon_t \sim N(0, \sigma_\kappa^2), \quad (3)$$

where δ is the drift parameter and ϵ_t are the error terms, normally distributed with null mean and variance σ_κ^2 .

3. Neural Network Model

The term neural network (NN) originated as a mathematical model that replicates the biological neural networks of the human brain (Minsky and Pitts (1943), Wiener (1948)). NN architecture includes neurons, synaptic connections that link the neurons, and learning algorithms. Typically, NN is formed by three types of layers, respectively, called input, hidden and output layer and each one has several neurons. Each unit in a network gets “weighted” information through synaptic links from the other connected ones and returns an output by using an activation function transforming the weighted sum of input signals.

Considering a single neuron H —called perceptron by Rosenblatt (1958)—its output is defined as:

$$out_H = \phi(\mathbf{w}^T \mathbf{x} + b), \quad (4)$$

where $\mathbf{x} \in \mathbb{R}^d$ is the input, $\mathbf{w} \in \mathbb{R}^d$ is the associate synaptic weight, $d \in \mathbb{N}$ is the number of input signals and ϕ is the activation function. The term $b \in \mathbb{R}$ represents the bias, also called activation threshold. It is important to notice that the function ϕ must be differentiable because the learning equations are gradient-based.

NN with a single layer cannot be used for nonlinear separable problems like XOR (Minsky and Papert (2017)) but the introduction of MultiLayer Perceptron (MLP) has inspired new structures of more powerful NNs that overcome this limitation. In the MLP, the neurons are predisposed on different layers and each unit is fully-connected with those of the previous layer.

The way in which the units are connected by synapses defines different types of networks. In the NN classical pattern (feedforward NN), the information moves from the input to the output layer in only one direction, while, in the Recurrent Neural Networks (RNNs), the information is processed cyclically using additional synapses such that the result of the elaboration process was reprocessed as input.

Figure 1 shows the typical feedforward NN representation. Every node of the graph represents a neuron, connected to each other by arcs representing the synapses. In the graph, the generic input, latent, and output variables are represented.

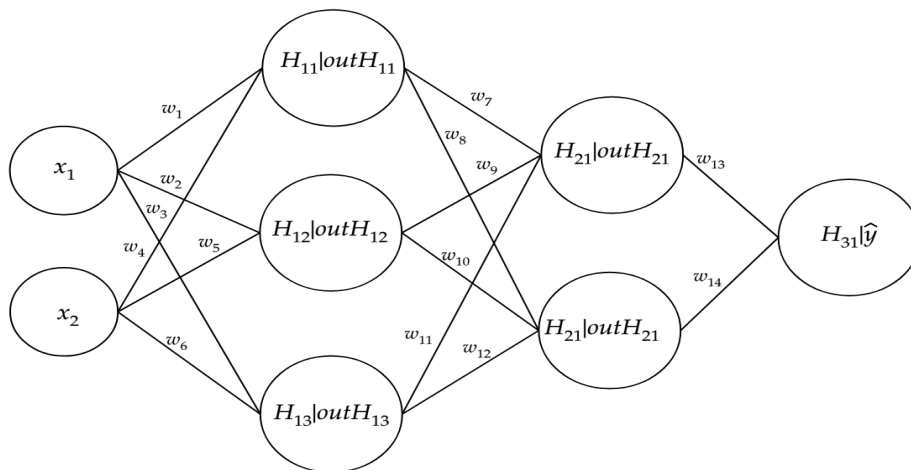


Figure 1. Schematical view of neural network (NN): the circles represent neurons and lines represent synapses. Synapses take the input and multiply it by a “weight” (the “strength” of the input in determining the output). Neurons add the outputs from all synapses and apply an activation function.

The output $\text{outH} \in \mathbb{R}^{n_h}$ of a generic hidden layer with n_h neurons is defined:

$$\text{outH} = \phi(W^T \mathbf{x} + \mathbf{b}), \tag{5}$$

where $W \in \mathbb{R}^{d \times n_h}$ is a weight matrix and $\mathbf{b} \in \mathbb{R}^{n_h}$ is a biases vector. In the MLP scheme, the output of a hidden layer becomes the input for the next layer.

Considering a regression problem, where $g \in \mathbb{N}$ is the number hidden layers, the output $\hat{y} \in \mathbb{R}$ is obtained by:

$$\begin{aligned} \text{outH}_1 &= \phi_1(W_1^T \mathbf{x} + \mathbf{b}_1), \\ \text{outH}_2 &= \phi_2(W_2^T \text{outH}_1 + \mathbf{b}_2), \\ &\dots \\ \hat{y} &= \phi_g(W_g^T \text{outH}_{g-1} + \mathbf{b}_g), \end{aligned}$$

where W_1, W_2, \dots, W_g are weight matrices, $\mathbf{b}_1, \mathbf{b}_2, \dots, \mathbf{b}_g$ are bias vectors, and $\phi_1, \phi_2, \dots, \phi_g$ are activation functions not necessarily different from each other. It is important to notice that the dimension of the weight matrices and the bias vectors depend on the number of units in the hidden layers. Increasing the number of hidden layers, the level of abstraction of the input data increases.

Back-propagation

NN training involves an unconstrained optimization problem where the aim is to minimize a function in high dimensional space. Let us define a loss function:

$$E = \frac{\sum (y - \hat{y})^2}{2} \tag{6}$$

that measures the difference between the predicted values \hat{y} and observed ones y . The quantity E depends on the matrices of the weights¹ W_1, W_2, \dots, W_g that influence the values of \hat{y} . The aim is to find the values of the synaptic weights that minimize the quantity E .

Among many other algorithms, the back-propagation is the most used for the training of feedforward NNs. The algorithm compares the predicted values against the desired ones (objective) and modifies the synaptic weights by back-propagating the gradient of the loss function. Schematically, the procedure alternates forward and backward propagation steps:

- in the forward step, the prediction \hat{y} are computed fixing the synaptic weights,
- in the backward step, the weights are adjusted in order to reduce the error E of the network.

The NN iteratively performs forward and backward propagation and modifies the weights to find the combination that minimizes the loss function.

Analytically, the back-propagation algorithm updates the weights W_g in the last layer using the delta rule (Bryson and Ho (1969)), defined as:

$$\Delta W_g = -r \frac{\partial E}{\partial W_g}, \tag{7}$$

where r is the learning rate. For the other previous layers, we proceed using the chain derivation rule. The updating of the weights matrix W_{g-1} are computed:

$$\Delta W_{g-1} = -r \frac{\partial E}{\partial \text{outH}_{g-1}} * \frac{\partial \text{outH}_{g-1}}{\partial W_{g-1}} \tag{8}$$

and so on for the other layers. In a figurative way, the idea behind the gradient descent is similar to “climbing down a hill” until a global or local minimum is reached. At each update, the search moves in the opposite direction of the gradient and the slope of the gradient and the learning rate determine the amplitude of this movement. In addition, the choice of the rate r is an important element, since a small value involves too many iterations while a large value could not allow convergence to the global minimum. Figure 2 shows the role of the learning rate in the convergence of the gradient descent in the simplest case of one-dimensional space.

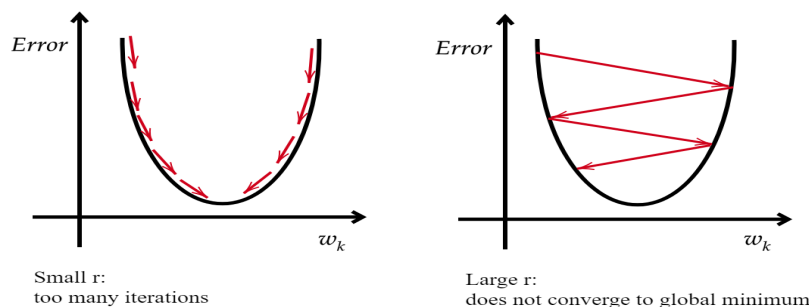


Figure 2. Rate of change and gradient descending.

¹ More precisely, E also depends on the biases vectors $\mathbf{b}_1, \mathbf{b}_2, \dots, \mathbf{b}_g$ of all hidden layers. For simplicity of notation, from now, for a generic layer $k \in [1, g]$, we indicate with W_k the complete matrix $(W_k^T | \mathbf{b}_k)^T$.

The choices concerning the type of architecture (e.g., the number of hidden layers, units for each layer) and the hyperparameter values (e.g., learning rate, activation function, epochs) remain a heuristic problem for NN users: the choice often depends on the type of data and it is not an easy step. A preliminary round of hyperparameters tuning, before the testing, is highly desired. An extensive description of NNs and back-propagation algorithm can be found in [Alpaydin \(2010\)](#), [Hastie et al. \(2016\)](#) and [James et al. \(2017\)](#).

3.1. Recurrent Neural Network with Long Short-Term Memory Architecture

The feedforward NNs, although representing a powerful analysis tool ([Hornik et al. \(1989\)](#)), are inadequate to effectively manage time sequences of data.

The recurrent connections between nodes, which characterized the RNNs, allow for having a dynamic analysis of sequential data. However, by using the RNN structure, we usually face the major problem of gradients vanishing, in which the weights change, and becoming that small very fast as to have no effect. Therefore, the network gradually loses its ability to learn from the past, becoming operationally inadequate for the analysis of long data sequences and for making good predictions. For this reason, the RNNs have only a short memory.

To overcome this problem, [Hochreiter and Schmidhuber \(1997\)](#) developed the so-called Long Short-Term Memory, LSTM. The LSTM is an RNN whose architecture is such that it allows for considering the relationships between the data of the sequence, even if this is long, eliminating the vanishing gradient problem. In this manner, the RNNs acquire both long- and short-memory, managing to generate great performance, also in a time series context. After the original work, the LSTM has undergone several improvements, as shown in ([Gers et al. \(1999\)](#)) and ([Gers, Schmidhuber \(2000\)](#)), and it is now possible to define a well-composed basic structure called vanilla LSTM.

Accordingly with Figure 3, the single LSTM unit, called LSTM block, is composed of three gates, their interactions and the resulting memory cell. The block receives as initial information flow the current input $x_t \in \mathbb{R}^d$, the previous short-term result $h_{t-1} \in \mathbb{R}^{n_h}$ and the previous state of (long-term) memory cell $c_{t-1} \in \mathbb{R}^{n_h}$. The information is elaborated by three gates (red circle), named, respectively, forget gate, input gate and output gate, and auxiliary NNs (blue circle) helpful in the regularization of information flow.

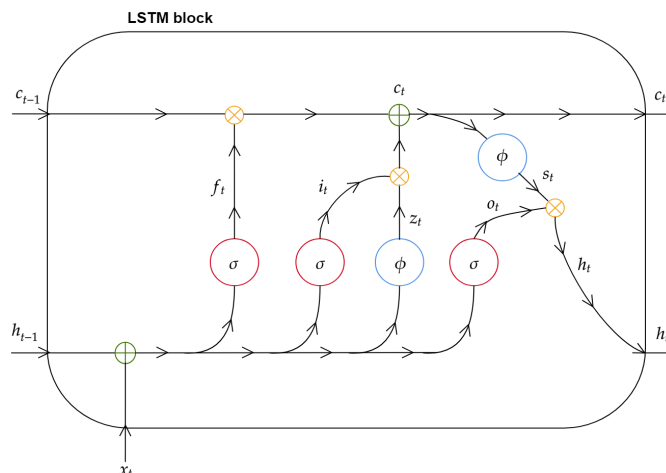


Figure 3. A representation of a vanilla Long Short-Term Memory (LSTM) block structure and its internal information forward flow.

Formally, referring to a hidden layer composed of $n_h \in \mathbb{N}$ of LSTM blocks, letting $W \in \mathbb{R}^{d \times n_h}$ and $U \in \mathbb{R}^{n_h \times n_h}$ weight matrices (for each gate) be respectively associated to the input and to the previous short

term result, the general mode of operation of a recurrent network with LSTM architecture is described by the following set of equations, specifying the forget gate output ($\mathbf{f}_t \in \mathbb{R}^{n_h}$), input gate output ($\mathbf{i}_t \in \mathbb{R}^{n_h}$), output of output gate ($\mathbf{o}_t \in \mathbb{R}^{n_h}$), and output of auxiliary-output gate ($\mathbf{z}_t \in \mathbb{R}^{n_h}$):

$$\mathbf{f}_t = \sigma(W_f \mathbf{x}_t + U_f \mathbf{h}_{t-1} + \mathbf{b}_f), \tag{9}$$

$$\mathbf{i}_t = \sigma(W_i \mathbf{x}_t + U_i \mathbf{h}_{t-1} + \mathbf{b}_i), \tag{10}$$

$$\mathbf{o}_t = \sigma(W_o \mathbf{x}_t + U_o \mathbf{h}_{t-1} + \mathbf{b}_o), \tag{11}$$

$$\mathbf{z}_t = \phi(W_z \mathbf{x}_t + U_z \mathbf{h}_{t-1} + \mathbf{b}_z). \tag{12}$$

The forget gate output \mathbf{f}_t , defined by Equation (9), is such that the information from the previous cell state and the one coming from the current input are mixed in a nonlinear way by a sigmoid activation function. Therefore, the output can assume value between 0 and 1, forgetting or keeping the state of the previous block. Afterwards, \mathbf{f}_t is mixed by a point-wise product with the previous state of memory \mathbf{c}_{t-1} .

The input gate \mathbf{i}_t , defined in Equation (10), also uses a sigmoid activation, allowing for deciding when information received should be updated.

The output gate \mathbf{o}_t , described in Equation (11), has the role to prevent the transmission of non-significant memory content stored information to the other blocks. For this purpose, a sigmoid function is used in order to pass relevant memory information. In order to regularize the flow of processed data, the input gate \mathbf{i}_t is combined with that obtained from the associated auxiliary NN \mathbf{z}_t as in Equation (12).

We define the processing of the entire input block, which participates in formulation of the current state of memory cell, as follows:

$$\mathbf{c}_t = \mathbf{c}_{t-1} \circ \mathbf{f}_t + \mathbf{i}_t \circ \mathbf{z}_t. \tag{13}$$

To obtain the current output, a combination between a function of \mathbf{c}_t , $\mathbf{s}_t = \phi(\mathbf{c}_t)$, and the upshot of auxiliary NN associated to output gate is necessary:

$$\mathbf{outH} = \mathbf{s}_t \circ \mathbf{o}_t. \tag{14}$$

The output $\mathbf{outH} \in \mathbb{R}^{n_h}$ is passed to the next layer and became the short memory $h_t = \mathbf{outH}$ for the next instance. The general mode of RNN operation with LSTM architecture at each time step is represented in Figure 4.

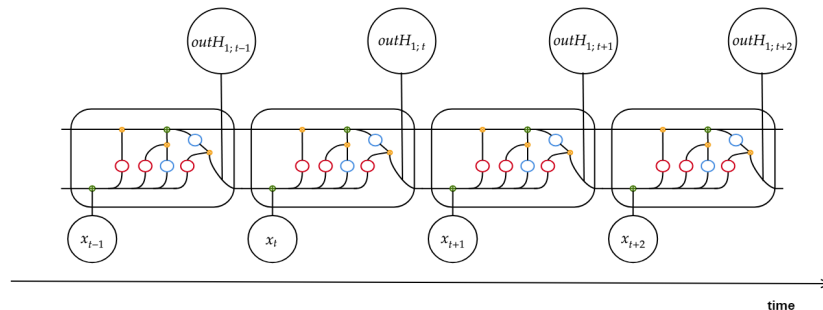


Figure 4. A simplified representation on sequential operation of a one-hidden layered Recurrent Neural Network (RNN) with LSTM architecture for each time step.

In light of the framework described above, we will show that the LSTM architecture is an excellent tool in the context of forecasting time series, especially in the case of very long time lag connections, as well as for catching and managing the noise. However, it is important to remind that the LSTM users, like those of NNs in general, have to face the classical problems concerning the choice of hyperparameters.

4. Numerical Application

In this section, we introduce the RNN with LSTM architecture in the classical scheme of the LC model. More precisely, our aim is to exploit the merits and functionalities of the LSTM architecture in order to improve the predictive capacity of the LC model. For this purpose, we design a set of experiments aimed to test the skills of LSTM in predicting the evolution of future mortality over time and to compare its performance with those derived from ARIMA.

Therefore, the analysis will concern the prediction of the time index k_t trend, considering the ARIMA model as forecast benchmark, while the parameters a_x and b_x are obtained according to the estimation procedure applied by Lee and Carter (1992).

Differently from the LC model that uses a random walk with drift, we calibrate the best ARIMA(p,d,q) according to the Hyndman–Khandakar algorithm (Hyndman, Khandakar (2008)). In the first round, the procedure checks the stationarity of the time series using an appropriate unit root test and chooses the differencing order d . In a second stage, it selects the best values of auto-regressive and moving average order, respectively p and q , using a specific information criteria (AIC or BIC). The algorithm is implemented by the function *auto.arima* available in the R package forecast (Hyndman, Khandakar (2008), Hyndman et al. (2019)).

The ARIMA performance is then compared to the LSTM one. The LSTM seems to be the more natural competitor of the ARIMA (p,d,q) model, for its ability to capture the long-term pattern inside the sequential data. We build a LSTM model that approximates the function f linking κ_t to its time lags, as follows:

$$\text{LSTM : } \kappa_t = f(\kappa_{t-1}, \kappa_{t-2}, \dots, \kappa_{t-J}) + \epsilon_t, \tag{15}$$

where $J \in \mathbb{N}$ is the number of time lags considered and ϵ is a homoschedastic error term.

LSTM network, like other machine learning techniques, requires the splitting of the dataset into training set and testing set. The training set stands for supervised learning, while the testing is used to validate the model. The supervised learning dataset (Table 1) is built as follows:

Table 1. Dataset for the supervised learning.

Output		Input		
κ_t	κ_{t-1}	κ_{t-2}	...	κ_{t-J}
κ_{t+1}	κ_t	κ_{t-1}	...	κ_{t-J+1}
κ_{t+2}	κ_{t+1}	κ_t	...	κ_{t-J+2}
...
κ_{t+n}	κ_{t+n-1}	κ_{t+n-2}	...	κ_{t-J+n}

After the training phase, the network has learned the input–output functional relationship and it should be able to predict future values of κ_t using only the input. In practice, the input is a $(n \times J)$ matrix of the time lags of κ_t and the output is the $(n \times 1)$ vector of its current values, where $n \in \mathbb{N}$ is the number of instances.

The forecasted values of κ_t , at time $n + 1, n + 2, \dots, n + J$, are carried out recursively. In general terms, the predicted value of $\hat{\kappa}_t$ in a generic time $n + \tau$ is calculated using the values of κ_t with $t = (n + \tau - 1, n + \tau - 2, \dots, n + \tau - J)$ as input. It is important to note that, going forward in the forecasting,

the future values of κ_t time index are calculated using only predicted values $\hat{\kappa}_t$ and not those observed. However, the forecasted data have not yet been observed, and the model’s accuracy becomes impossible to be measured.

The year T , which corresponds to the last observation in training set, is the starting point for forecasting. Therefore, we consider $T < n$, where the observations before T represent the training set and the remaining $n - T$ form the testing set.

All experiments has been run with R version 3.5.2 (R Foundation for Statistical Computing, Vienna, Austria. <http://www.R-project.org/>), using the keras, tensorflow, mlr (Bischl et al. (2016)), demography (Hyndman (2019)) and HMDHFDplus packages for the selected models. In addition, the package ggplot2 has been used for the results’ visualization.

The analysis is carried out on six countries, Australia, Denmark, Italy, Spain, the U.S.A. and Japan, and data are taken from the Human Mortality Database (HMD). This database provides mortality rates, number of deaths and exposures for different ages and different countries distinguishing by gender. The whole period available in HMD has been considered for each country and the analysis has been performed considering one time lag ($J = 1$).

The first step is to estimate the LC model parameters a_x , b_x and κ_t using an SVD. The extracted time series of κ_t represent the initial base for the analysis. These data are split into training and testing set according to the rule of 80% training and 20% testing. Therefore, the last year T of observation is consequentially determined. The total available years and the corresponding testing set years considered in the analysis are shown in Table 2 by country. The age range is set to 0–100.

Table 2. Total and testing set years by country.

Country	Total Years	Testing Set Years
Australia	1921–2014	1996–2014
Denmark	1835–2016	1981–2016
Italy	1872–2014	1987–2014
Spain	1908–2016	1995–2016
U.S.A.	1933–2016	2001–2016
Japan	1947–2016	2003–2016

In order to select the best combination of hyperparameters for the network, a preliminary round of fine-tuning is carried out for all countries, distinguishing by gender. The best combinations, obtained in this step, are used for the LSTM calibration in the forecasting procedure.

About the results of the tuning, we have noticed that the architectures with a single hidden layer work better than the others on our data and the number of neurons depends on the country. The Rectified Linear Unit (ReLU) activation function outperformed the other functions tested for all countries. In addition, no clear evidence emerged for the influence of other hyperparameters on the performance.

About the calibration of the ARIMA(p,d,q) model, Table 3 shows the best specification for each country distinguished by gender.

Table 3. Best ARIMA for each country and each gender.

Country	Best ARIMA(p,d,q)
<i>Australia</i>	
Male	ARIMA (1,1,0)
Female	ARIMA (1,1,0)
<i>Denmark</i>	
Male	ARIMA (0,1,3)
Female	ARIMA (0,1,3)
<i>Italy</i>	
Male	ARIMA (0,1,3)
Female	ARIMA (0,1,1)
<i>Spain</i>	
Male	ARIMA (1,1,0)
Female	ARIMA (1,1,0)
<i>U.S.A.</i>	
Male	ARIMA (0,1,0)
Female	ARIMA (0,1,0)
<i>Japan</i>	
Male	ARIMA (0,1,3)
Female	ARIMA (0,1,3)

Following the calibration step, the analysis includes numerical and graphical processing of the goodness of fit. In particular, we follow the out of sample approach that represents the testing step in the machine learning field. Concerning graphical analysis, Figures 5 and 6 show the κ_t parameter estimation obtained from SVD, respectively for male and female. The dashed vertical line separates the forecasted period from the one used to train the LSTM network. For the ARIMA models, we also show the confidence interval with 0.995 confidence level.

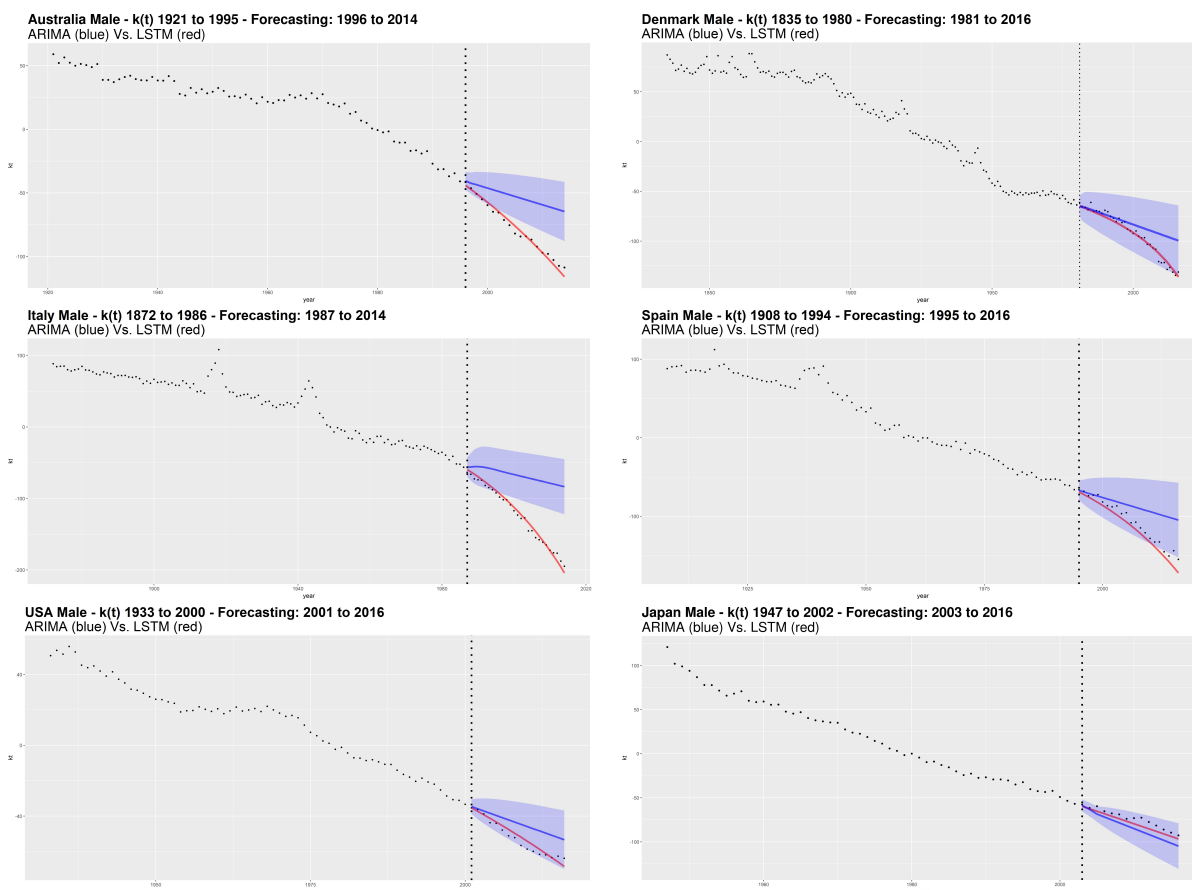


Figure 5. Historical and forecasted values of κ_t for male population.

Besides graphical check, to compare the performance of LSTM against the best ARIMA in the testing set and measure the forecasting quality, we calculate the following goodness of fit measures:

$$\text{Mean Absolute Error (MAE): } \frac{\sum_{\tau=T+1}^{n-T} |\kappa_{\tau} - \hat{\kappa}_{\tau}|}{(n - T)}, \tag{16}$$

$$\text{Root Mean Square Error (RMSE): } \sqrt{\frac{\sum_{\tau=T+1}^{n-T} (\kappa_{\tau} - \hat{\kappa}_{\tau})^2}{(n - T)}}. \tag{17}$$

Table 4 shows the performance of LSTM and ARIMA in terms of RMSE and MAE, by country and gender.

From the κ_t plots and the results of goodness of fit measures, we observe that the LSTM network provides the best performances compared to the ARIMA model.

Considering the error measures, MAE and RMSE, Italy shows the best LSTM performance with respect to the ARIMA for both genders. Also by a graphical analysis, the LSTM seems to catch very well the nonlinearity of the future mortality trend showing its remarkable ability to better represent the decreasing dynamics of mortality, with respect to the ARIMA model. The “worst” LSTM performance is obtained for Japan male and Denmark female, but still winning compared to the ARIMA.

More generally, we notice a higher capacity of the LSTM to capture nonlinear trends without incurring in the opposite situation, that is, an excessively oscillating or excessively parabolic trend (the latter observed in the traditional NNs). On the other hand, our analysis shows that ARIMA is not effective. The evolution

of κ_t according to the ARIMA models is sometimes even outside of the confidence interval, like in the case of Italy (both genders), Australia (male) and Spain (female).

Table 4. Performance of Long Short-Term Memory (LSTM) and ARIMA in the testing set for each country.

Country	Male		Female	
<i>Australia</i>	<i>MAE</i>	<i>RMSE</i>	<i>MAE</i>	<i>RMSE</i>
κ_t ARIMA	24.75	28.04	13.95	15.55
κ_t LSTM	2.57	3.24	3.12	3.83
<i>Denmark</i>	<i>MAE</i>	<i>RMSE</i>	<i>MAE</i>	<i>RMSE</i>
κ_t ARIMA	11.10	16.10	7.99	10.70
κ_t LSTM	2.97	3.84	6.62	8.18
<i>Italy</i>	<i>MAE</i>	<i>RMSE</i>	<i>MAE</i>	<i>RMSE</i>
κ_t ARIMA	55.41	63.46	41.12	45.74
κ_t LSTM	4.63	5.48	8.04	10.69
<i>Spain</i>	<i>MAE</i>	<i>RMSE</i>	<i>MAE</i>	<i>RMSE</i>
κ_t ARIMA	20.24	26.33	26.10	33.95
κ_t LSTM	7.69	8.96	15.61	17.67
<i>the U.S.A.</i>	<i>MAE</i>	<i>RMSE</i>	<i>MAE</i>	<i>RMSE</i>
κ_t ARIMA	8.39	9.48	10.81	12.54
κ_t LSTM	2.31	2.86	3.32	4.18
<i>Japan</i>	<i>MAE</i>	<i>RMSE</i>	<i>MAE</i>	<i>RMSE</i>
κ_t ARIMA	9.61	10.50	15.12	17.52
κ_t LSTM	4.71	5.24	7.89	10.23

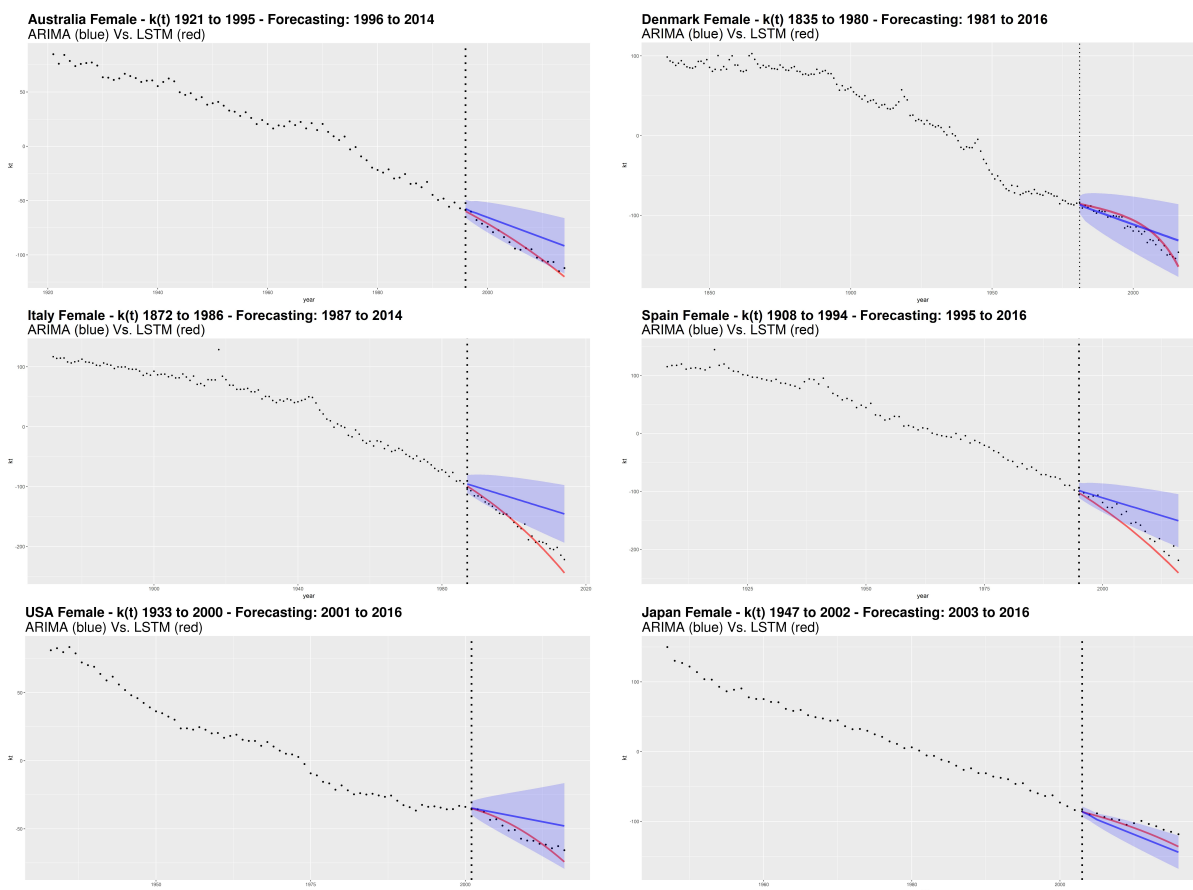


Figure 6. Historical and forecasted values of κ_t for female population.

Our results highlight the inadequacy of ARIMA to detect the decreasing dynamics of mortality over time. Although the ARIMA process is widely used in modeling the time indexes of mortality, it has a fixed structure and works well when data satisfies the ARIMA assumptions, e.g., the constant variance assumption that is one of the most important features of the integrated models. In many cases, demographical data may exhibit volatility changes and this feature does not fit the ARIMA assumption, especially for long time series.

Although NN is a very powerful learning algorithm, it only provides point predictions without any indication of their variability. Confidence intervals prediction is a real challenge in the NN field. The literature on this topic is not extensive and the question is still open. Some scholars (Khosravi et al. (2011), Keren et al. (2019)) have faced this problem, but none of them has so far treated the question concerning NNs (and more generally deep learning) applied to time series. However, the LSTM network demonstrates being a good candidate to meet the need of predicting the mortality trend over time more accurately. We can state that LSTM overperforms the ARIMA model in all of the analyzed countries thanks to its architecture that allows for learning well the significant influence from the past mortality and replaces it with high precision for future years. This ability of LSTM network is noticeable, especially for populations where κ_t parameter does not have a prominent linear trend.

Another remarkable aspect of LSTM concerns the possibility to achieve a good forecasting performance without resorting to a priori selection of the time steps. By way of example, we show the predicted values of life expectancy (Figure 7), death distribution $D_{x,t}$ (Figure 8) and log-mortality rates $\log(m_{x,t})$ (Figure 9) obtained by both models for Australian males. All of the analyses presented here

support the basic finding of an evident increase in life expectancy over time, as shown in the case of life expectancy at birth (Figure 7, left side). The ARIMA model provides a trivial shape of forecasted trend. The straight line of future k_t values, constant over time, produces an unrealistic behavior of the forecasted mortality shape. Conversely, the LC model integrated with LSTM produces a negligible gap between the real and forecasted values of life expectancy. From the results of $D_{x,t}$ and $\log(m_{x,t})$ depicted respectively in Figures 8 and 9 using a smoothed shape, we can confirm that LSTM provides a better prediction on real data, respect to the ARIMA model.

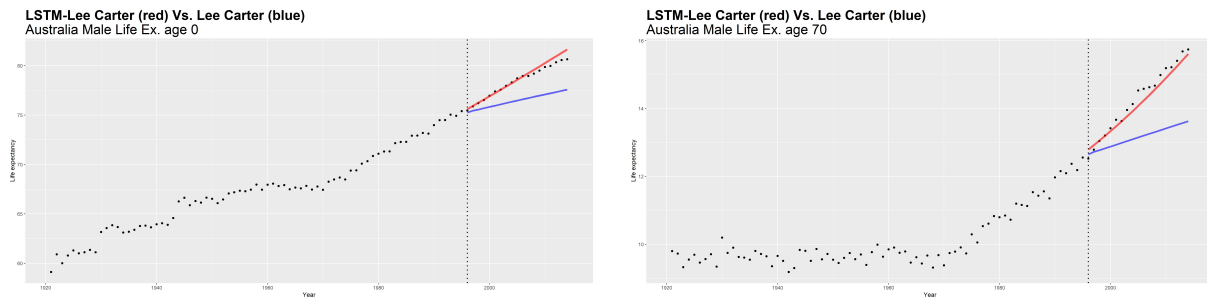


Figure 7. Life expectancy at birth (on the left) and at age 70 (on the right): ARIMA(1,1,0) vs. LSTM. Australian male population.

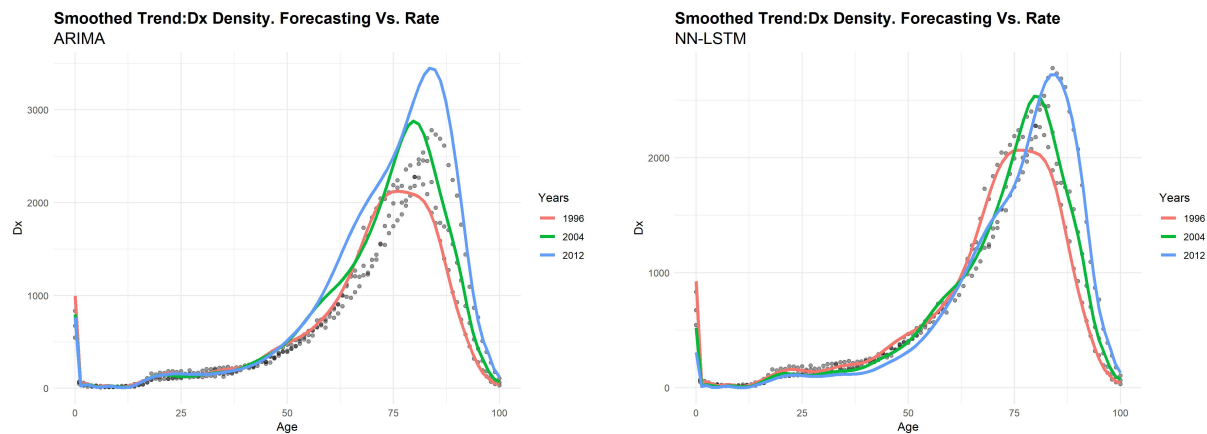


Figure 8. Distribution of deaths: ARIMA(1,1,0) (on the left) vs. LSTM (on the right). Australian male population.

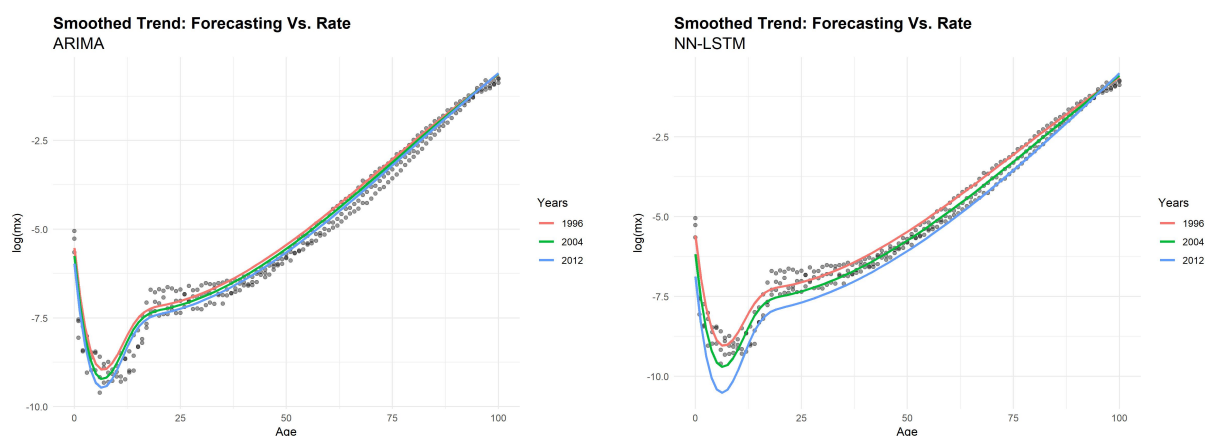


Figure 9. Logarithm of central death rates: ARIMA(1,1,0) (on the left) vs. LSTM (on the right). Australian male population.

5. Conclusions

In the mortality field, theories that embrace the steady increase in life expectancy have been extensively presented. In light of that, we can assert that mortality improvement is a fact. The shape of its pace remained a matter of debate. The latter point has an important reflection in the forecasting approach as well. For this reason, the field of nonlinear estimation of the time-dependent parameter in the LC model should represent a crucial point. Unfortunately, scholars have always focused efforts on enhancing LC fitting, overlooking a very important perspective: the forecasting trend.

In the present work, we have proposed a deep learning integrated LC model based on an RNN with LSTM architecture for the forecasting of the future values of k_t index. The investigation has been performed on six countries throughout the world and by gender. The proposed approach shows very high accuracy levels of the mortality trend forecast, compared to the canonical ARIMA. Indeed, the LSTM stores excellent performance thanks to its architecture, consisting of three steps: catching, memorizing and replicating. These features allow the LSTM to provide more accurate forecasting, according to the decreasing trend of mortality over time, than the best ARIMA process.

Moreover, it can be noticed that the LSTM power is evident in the life expectancy trend and death distribution as well, in which, thanks to “out of sample” scheme, you can see the tangible impact on demographic forecasting of a new way of thinking that uses innovative forecast tools. The classical LC model, as well as other mortality models that use an ARIMA process, can produce a trivial shape of the forecasted trend, which provides a constant behavior of the forecasted mortality shape over time. The LSTM, catching a more realistic nonlinearity behavior, makes it possible to emphasize the differences between real and predicted values over time. In particular, concerning the life expectancy shape provided by the LC model integrated via LSTM, the discrepancy between the real value of the time series and the forecasted one is minimal. Our model provides a more optimistic scenario about mortality, in accordance with the widely accepted hypothesis of a constant increase in life expectancy.

This evidence supports the usefulness of the deep learning integration of the LC model proposed in the present work, which provides much more accurate predictions but at the same time preserves the LC advantages as parsimony and robustness. This last feature is particularly appreciated by the practitioners in life insurance industry, pension plans and social security schemes that have to compute and manage future cash flows, closely related to longevity dynamics. Since LSTM, and an NN in general, is a flexible tool, it is possible to overcome the ARIMA restrictions and conduct a more realistic evaluation. It is important to remember that the approach proposed in this paper provides point prediction, while the

analysis of variability and the construction of confidence intervals remain an actual challenge in the NN field.

In a future work, we plan to extend the analysis to other countries included in the HMD database and explore the potentiality of the LSTM in other stochastic mortality models. In our opinion, the analysis of the variability and robustness of the LSTM (and machine learning models in general) remains one of the most important points in the field of data science and machine learning techniques (Richman and Wüthrich (2018)), which might be worth facing.

Author Contributions: Conceptualization, A.N.; methodology, A.N., M.M. and S.S.; formal analysis, A.N., M.M. and S.S.; writing—original draft preparation, A.N. and S.L.; writing—review and editing, A.N., S.L., M.M., S.S. and F.P.; visualization, A.N.; supervision, S.L. and F.P.

Funding: This research received no external funding.

Acknowledgments: The authors would like to thank the anonymous referees for helpful comments.

Conflicts of Interest: The authors declare no conflict of interest.

References

- Alpaydin, Ethem. 2010. *Introduction to Machine Learning*, 2nd ed. Cambridge: Massachusetts Institute of Technology Press.
- Bischi, Bernd, Michel Lang, Lars Kotthoff, Julia Schiffner, Jakob Richter, Erich Studerus, Giuseppe Casalicchio, and Zachary M. Jones. 2016. mlr: Machine Learning in R. *Journal of Machine Learning Research* 17: 5938–5942.
- Bryson, Arthur Earl, and Yu-Chi Ho. 1969. *Applied Optimal Control*. Waltham: Blaisdell.
- Brouhns, Natacha, Michel Denuit, and Jeroen K. Vermunt. 2002. A Poisson log-bilinear regression approach the construction of projected lifetables. *Insurance: Mathematics and Economics* 31: 373–393.
- Castellani, Gilberto, Ugo Fiore, Zeldia Marino, Luca Passalacqua, Francesca Perla, Salvatore Scognamiglio, and Paolo Zanetti. 2018. An investigation of Machine Learning Approaches in the Solvency II Valuation Framework. Available online: https://papers.ssrn.com/sol3/papers.cfm?abstract_id=3303296 (accessed on 1 March 2019).
- Deprez, Philippe, Pavel V. Shevchenko, and Mario V. Wüthrich. 2017. Machine learning techniques for mortality modeling. *European Actuarial Journal* 7: 337–352.
- Gabrielli, Andrea, and Mario V Wüthrich. 2018. An Individual Claims History Simulation Machine. *Risks* 6: 29.
- Gers, Felix Alexander, and Jürgen Schmidhuber. 2000. Recurrent nets that time and count. Paper presented at IEEE-INNS-ENNS International Joint Conference on Neural Networks, Como, Italy July 24–27, pp. 189–194.
- Gers, Felix Alexander, Jürgen Schmidhuber, and Fred Cummins. 1999. Learning to forget: Continual prediction with LSTM. *Artificial Neural Networks* 470: 850–855.
- Hainaut, Donatien. 2018. A neural-network analyzer for mortality forecast. *Astin Bulletin* 48: 481–508.
- Trevor, Hastie, Tibshirani Robert, and Friedman Jerome 2016. *The Elements of Statistical Learning. Data Mining, Inference, and Prediction*, 2nd ed. Springer. ISBN 10: 0387848576. New York. Doi:10.1007/978-0-387-84858-7
- Hochreiter, Sepp, and Jürgen Schmidhuber. 1997. Long Short-Term Memory. *Neural Computation* 9: 1735–1780.
- Hornik, Kurt, Maxwell Stinchcombe, and Halbert White. 1989. Multilayer feedforward networks are universal approximators. *Neural Networks* 2: 359–366. Doi:10.1016/0893-6080(89)90020-8.
- Human Mortality Database. University of California, Berkeley (USA) and Max Planck Institute for Demographic Research (Germany). Available online: <http://www.mortality.org> (accessed on 1 December 2018).
- Hyndman, Rob John. 2019. Demography: Forecasting Mortality, Fertility, Migration and Population Data. Available online: <https://cran.r-project.org/package=demography> (accessed on 20 January 2018).
- Hyndman, Rob John, George Athanasopoulos, Christoph Bergmeir, Gabriel Caceres, Leanne Chhay, Mitchell O’Hara-Wild, Fotios Petropoulos, Slava Razbash, Earo Wang, and Farah Yasmeen. 2019. Forecast: Forecasting Functions for Time Series and Linear Models. R package Version 8.5. Available online: <http://pkg.robjhyndman.com/forecast> (accessed on 31 December 2018).

- Hyndman, Rob John, and Yeasmin Khandakar. 2008. Automatic time series forecasting: the forecast package for R. *Journal of Statistical Software* 26: 1–22.
- James, Gareth, Daniela Witten, Trevor Hastie, and Robert Tibshirani. 2017. *An Introduction to Statistical Learning: with Applications in R*. Springer Texts in Statistics. Springer. ISBN 10: 1461471370. New York. Doi:10.1007/978-1-4614-7138-7.
- Khosravi, Abbas, Saeid Nahavandi, Doug Creighton, and Amir Atiya. 2011. A Comprehensive Review of Neural Network-based Prediction Intervals and New Advances. *IEEE Transactions on Neural Networks* 22: 1341–1356.
- Keren, Gil, Nicholas Cummins, and Björn Schuller. 2019. Calibrated Prediction Intervals for Neural Network Regressors. *Access IEEE* 6: 54033–54041.
- Lee, Ronald Demos, and Lawrence Carter. 1992. Modeling and forecasting US mortality. *Journal of the American statistical association* 87: 659–671.
- Levantesi, Susanna, and Virginia Pizzorusso. 2018. Application of machine learning to mortality modeling and forecasting. *Risks* 7: 26.
- Li, Johnny Siu-Hang, Mary R. Hardy, and Ken Seng Tan. 2009. Uncertainty in Mortality Forecasting: An Extension to the Classical Lee–Carter Approach. *ASTIN Bulletin* 39: 137–164.
- McCulloch, Warren S., and Walter Pitts. 1943. A logical calculus of the ideas immanent in nervous activity. *Bulletin of Mathematical Biophysics* 5: 115–133.
- Minsky, Marvin, and Seymour Papert. 2017. *Perceptrons Reissue of the 1988 Expanded Edition with a new Foreword by Léon Bottou*. Cambridge: Massachusetts Institute of Technology Press. ISBN 9780262534772.
- Oeppen, Jim, and James Walton Vaupel. 2002. Broken Limits to Life Expectancy. *Science* 296: 1029–1031.
- Richman, Ronald, and Mario V. Wuthrich. 2018. A Neural Network Extension of the Lee–Carter Model to Multiple Populations. Available online: https://papers.ssrn.com/sol3/papers.cfm?abstract_id=3270877 (accessed on 20 November 2018).
- Rosenblatt, Frank. 1958. The Perceptron: A Probabilistic Model for Information Storage and Organization in the Brain. *Psychological Review* 65: 386–408.
- Wiener, Norbert. 1948. *Cybernetics: or Control and Communication in the Animal and the Machine*, 2nd ed. Cambridge: Massachusetts Institute of Technology Press.



© 2019 by the authors. Licensee MDPI, Basel, Switzerland. This article is an open access article distributed under the terms and conditions of the Creative Commons Attribution (CC BY) license (<http://creativecommons.org/licenses/by/4.0/>).